Influence of Polyethylene-like Short-Range Intramolecular Interactions on the Segregation of Short Branches and Growth of the Interfacial Region in Simulations of Lightly Branched Semicrystalline Polymers

Klein Rodrigues, Saubhagya C. Mathur, and Wayne L. Mattice*

Institute of Polymer Science, The University of Akron, Akron, Ohio 44325-3909.
Received September 1, 1989; Revised Manuscript Received November 28, 1989

ABSTRACT: The amorphous region of a semicrystalline polymer with a few short branches has been simulated on a cubic lattice, with all sites singly occupied and with the inclusion of first- and second-order intramolecular interactions. The first-order interaction contributes an energy of E_σ for each pair of consecutive bonds that make an angle of 90°. The second-order interaction contributes an energy of E_ω when two consecutive bond angles are 90° and the dihedral angle is 0° at the bond common to these bond angles. Each branch occupies two lattice sites, and as many as 2% of the beads are trifunctional branch points. The segregation of the short branches in the layers near the crystal surface is not very sensitive to assignments in the range $0.54 < \sigma < 1$ and $0.54 < \omega < 1$, where $\sigma = \exp(-E_\sigma/RT)$ and $\omega = \exp(-E_\omega/RT)$. In contrast, the growth of the anisotropic interfacial region accompanying this segregation becomes more dramatic as σ decreases and, to a lesser extent, as ω decreases.

Introduction

Copolymers of ethylene with a small amount of a larger 1-alkene make up a growing fraction of the production of polyethylene.[1] These semicrystalline polymers are of special interest because their properties are modified in useful ways by the short branches from the 1-alkene comonomer. The methyl branches contributed by propene can be accommodated in the crystalline structure of polyethylene,[2-6] but the short branches contributed by larger 1-alkenes are excluded from the crystalline regions.[6,7] The greatest interest lies in ethylene–1-alkene copolymers in which the short branches are larger than methyl. Consequently the development of a molecular explanation for the influence of the short branches on useful properties has as a prerequisite the understanding of the distribution of the short branches in the amorphous region and the consequences of the presence of these short branches for the conformational properties of those chain segments that lie in this region.

The influence of the short branches on the amorphous region of a semicrystalline polymer has been investigated using square[8] and cubic[9] lattices on which every site is singly occupied. These lattices enforce bond angles and dihedral angles that are different from those found in polyethylene, but they offer the very important advantage of efficient simulation of a disordered system at bulk density. The simulations reported previously[8,9] weighted equally every configuration of the lattice in which every site was singly occupied and no chains were cyclic. Three important conclusions emerged from these simulations.[8,9] First, the smallest short branches (each consisting of a single step on the lattice) were randomly distributed throughout the amorphous region, but longer short branches had a decidedly nonrandom distribution. The longer short branches occurred preferentially in the anisotropic interfacial region, between the crystal and the isotropic region. Second, the segregation of the short branches in the anisotropic interfacial region was accompanied by a growth of this region at the expense of the isotropic amorphous region. Third, segregation of the short branches was also accompanied by an increase in the formation of tight folds, in order to avoid the increase in density of the interfacial region that would otherwise arise from the addition of the atoms in the short branches. The important role of the maintenance of bulk density in the amorphous region on the content of tight folds has been identified earlier in the investigation of semicrystalline polymers that have no short branches.[10]

The present objective is to determine the connection between the short-range intramolecular interactions and the influence of the short branches on the amorphous region. In particular, the focus is on short-range interactions that exercise a preference for rotational isomers that favor chain extension and penalize those combinations of successive rotational isomers that produce a reversal in the direction of the chain. These short-range interactions are of special interest because unperturbed polyethylene[11] has a preference for trans states over gauche states and must pay a severe energetic penalty when two successive bonds adopt gauche placements of opposite sign, a conformation important in the formation of a tight fold.

This approach shows that the segregation of the short branches is relatively insensitive to the intramolecular short-range interactions, but the growth of the anisotropic interfacial region as a consequence of branch segregation is strongly influenced by the short-range interactions. A preliminary description of the results has been presented elsewhere.[12]

Simulation

All simulations were performed using the system described earlier[8] but with the inclusion of the short-range intramolecular interactions. The method is summarized briefly here. In the absence of any short branches, the simulation uses the methodology developed by Mansfield[13,14] for the investigation of the amorphous region of a semicrystalline polymer, modeled on a cubic lattice with all sites singly occupied. Our cubic lattice is of dimensions $7 \times 7 \times 30$. The longer dimension, which is taken to be in the z direction, is normal to the planes of the two crystal surfaces. One crystalline lamella lies below $z = 1$, and the other crystalline lamella is above $z = 30$. Periodic boundary conditions are used in the x and y directions. The "bond-flip", with prohibition of the formation of a cyclic chain, as described by Mansfield, was

0024-9297/90/2223-2484$02.50/0

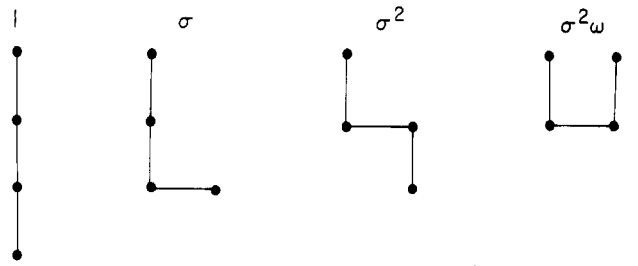

Figure 1. Four conformations of a chain segment with three bonds in conformations with statistical weights of 1, σ, σ^2, and $\sigma^2\omega$, reading from left to right.

used to convert the lattice from one configuration to another. When short branches were present, the algorithm prohibits a bond-flip that would change the number of bonds in a short branch.[8,9] Two special moves, end attack and simultaneous creation/destruction,[8,9] were used to change the positions of attachment of the short branches and the location of the atoms in the short branches. The moves did not change the number of short branches on the lattice nor the number of lattice sites in a short branch.

In the previous simulations, a proposed new configuration of the lattice was accepted if it maintained bulk density without voids or double occupancy, did not create a cyclic chain, and did not change the number of bonds in a branch.[8,9] In the present simulations, a new configuration that would previously have been automatically accepted is now conditionally accepted, using the Metropolis rules[15] and the change in the sum of the intramolecular short-range energies for all chains on the lattice.

Results and Discussion

The two types of terms that contribute to the intrachain energy are described with the aid of Figure 1. The zero of energy is assigned to the fully extended chain. On the cubic lattice, this conformation is a straight line. Each pair of consecutive bonds connected by a bond angle of 90° contributes an energy denoted by E_σ and a statistical weight $\sigma = \exp(-E_\sigma/RT)$. When this interaction is the only one present, the energy of a chain is determined solely by the number of 90° bond angles within it. The sequential arrangement of these 90° bond angles is irrelevant (except that it cannot produce a self-intersection of the chain). The sequence becomes important for the other energetic parameter, E_ω, and statistical weight, $\omega = \exp(-E_\omega/RT)$. An energy of E_ω is contributed by each triplet of successive bonds in which both bond angles are 90°, and the dihedral angle at the internal bond is 0°, giving a cis placement.

E_σ and σ are analogous to the terms of the same designation in the rotational isomeric treatment of unperturbed polyethylene[11] in that they reflect a local bias for an extended conformation and, by themselves, produce a chain in which the bonds are independent. The interdependence of the short-range interactions is brought into play via E_ω and ω and in a way that penalizes local conformations that produce the tightest bends. The analogy between the terms used in rotational isomeric state theory and those used here is not exact, as is immediately obvious from consideration of the number of local conformations that are weighted with σ. In the rotational isomeric state chain, two gauche conformations are weighted by σ, relative to the trans conformation, but on the cubic lattice four conformations with a bond angle of 90° are weighted by σ relative to the conformation with a bond angle of 180°.

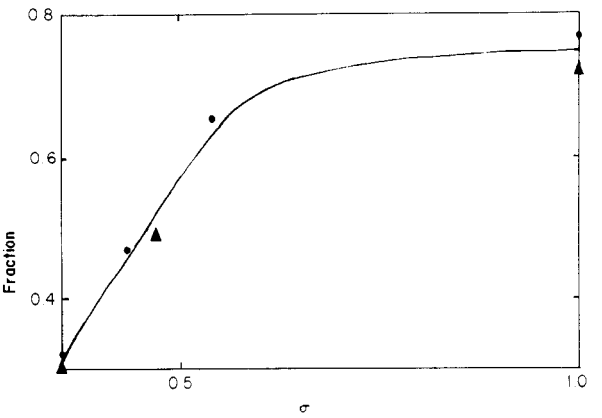

Figure 2. Fraction of emergent stems that form tight folds, as a function of σ, when $\omega = 1$. Circles denote the present results, and triangles are results obtained by Mansfield.[14] The solid line is drawn by eye to follow the pattern suggested by the circles and triangles.

Figure 2 depicts the content of tight folds, as a function of σ, in simulations performed on systems that contained no branches. The value of ω is 1 throughout. Also plotted on the figure are the results for three simulations performed by Mansfield.[14] When $\sigma = 1$, the content of tight folds is 0.72 and 0.77 from the two simulations. As σ decreases, the content of tight folds also decreases, reaching 0.31 ± 0.01 in the simulations with $\sigma = 0.36$. The same trend is depicted by the circles and the triangles in Figure 2, but there is a slight tendency for the present simulations to give a higher content of tight folds than that reported by Mansfield.

Measures of Branch Size and Branch Content. Each simulation with branches is performed for a system in which the number and size of the short branches is constant. The size of the short branch is given by the number of lattice sites and is denoted by n_b.

The content of short branches is specified by the fraction of lattice sites that are trifunctional branch points. This fraction is denoted by $f_{b,a}$, where f_b is the fraction of sites that are trifunctional branch points, and the additional subscript "a" specifies that the evaluation is for the amorphous region only. This specification must be appended, because the lattice is used only for the simulation of the amorphous region. The crystal is not simulated because the conformation of the chains within it is known, and the short branches of greatest interest are excluded from the crystalline region. For the macroscopic sample, the fraction of chain atoms that are trifunctional branch points, f_b (only a single subscript), is

$$f_b = f_{b,c}f_c + f_{b,a}(1 - f_c) \quad (1)$$

where $f_{b,c}$ is the fraction of the chain atoms in the crystalline region that are trifunctional branch points and f_c is the fraction of the material that is crystalline. If the short branches are excluded from the crystal, $f_{b,c}$ is negligibly small, and the expression for f_b reduces to

$$f_b = f_{b,a}(1 - f_c) \quad (2)$$

In the simulations reported here, the values of $f_{b,a}$ range from 0 to 0.02. Conversion of $f_{b,a}$ to the macroscopic branch content, f_b, should be performed via eq 2. Consequently the value of $f_{b,a}$ is not related in a unique manner to the macroscopic f_b. Instead, $f_{b,a}$ is related to f_b by a process that includes a consideration of the conditions used for crystallization and hence the value for f_c. Since f_c must be larger than 0 if the sample is at all crystalline (as we assume it is), it is clear that $f_b < f_{b,a}$. The absence of a value of f_c causes no difficulty in the performance of the

Table I
Distribution of Branches in Chains on the Lattice When $f_{b,a} = 0.02$ and $l_z = 30$

probabilities	value[a]	range[b]
p_0	0.545	$0.39 < p_0 < 0.98$
p_1	0.334	$0 \le p_1 < 0.61$
p_2	0.099	$0 \le p_2 < 0.31$
p_3	0.026	$0 \le p_3 < 0.20$
p_4	0.003	$0 \le p_4 < 0.14$
p_5	0.000	$0 \le p_5 < 0.12$
$1 - p_0 - p_1$	0.121	
$(1 - p_0 - p_1)/(1 - p_0)$	0.266	

[a] Values when all chains have the same contour length. [b] Upper and lower limits for chains with any combination of contour lengths.

simulation, because Mansfield's method does not require a specification of the size of the crystalline region or the degree of crystallization, except that f_c cannot be zero.

The probability, p_i, that a chain on the lattice contains i short branches is easily evaluated in the approximation that each such chain is assigned a contour length identical with the average contour length. The average contour length is simply the number of lattice steps in the z direction, l_z, which has a value of 30 in the present case. Then

$$p_i = \{l_z![(l_z - i)!i!]^{-1}\} f_{b,a}{}^i (1 - f_{b,a})^{l_z - i} \quad (3)$$

Numerical results for p_i for the present simulations, evaluated using $f_{b,a} = 0.02$, are presented in Table I. Even at the highest branch density used in the present work, the majority of the chains in the amorphous region are not expected to contain a branch. Under these same conditions, only $^1/_8$ of the chains are expected to contain two or more branches. (This fraction falls to $^1/_{30}$ when $f_{b,a} = 0.01$.) Of those chains that do contain one or more branches, about $^3/_4$ contain only a single branch and only $^1/_4$ contain multiple branches.

Of course, an amorphous region will not contain chains that all have the same contour length but will instead contain chains with a variety of contour lengths. The last column in Table I gives the range for the p_i for any conceivable distribution of short branches. In the case of p_0, the lower limit of 0.39 is obtained when no chain can have more than one branch. In this case, p_1 is 0.61, and the p_i, $i > 1$, are all zero. The upper limit for p_0, 0.98, is obtained in the extremely unlikely case where all of the short branches are on a single chain. The maximum occurrence of chains with multiple branches is obtained in the unusual distribution where every chain contains either exactly two branches or no branches at all. In this case, p_0 is 0.69 and p_2 is 0.31. Typical distributions of short branches over the chains in the amorphous region should be closer to that described in the second column of Table I than to the outer limits specified in the last column. Most of the chains contain a single short branch or no branches at all.

Segregation of Short Branches. Previous simulations, performed with $\sigma = \omega = 1$, have shown that short branches with $n_b = 1$ have a nearly random distribution in the lattice, but short branches with $n_b = 2$ have a decidedly nonrandom distribution.[8,9] Curves denoted by filled circles in Figures 3 and 4 depict the distribution of the trifunctional branch points and the branch ends, respectively, when $n_b = 2$ and $f_{b,a} = 0.02$. The representation is as the fraction of the beads that are trifunctional branch points, or branch ends, as a function of the distance of the layer, measured in lattice steps, from the nearest crystal surface. Thus layer 1 in these figures is the layer adjacent to the crystal, and layer 15 is the layer furthest from the crystal. The horizontal dashed line at a fraction of

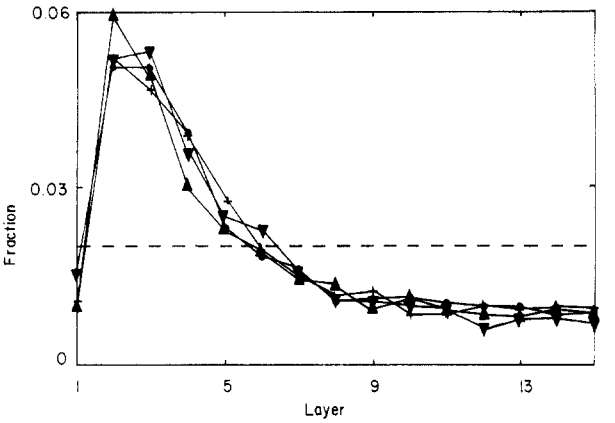

Figure 3. Fraction of lattice sites in each layer that are occupied by a trifunctional branch point when $n_b = 2$, $f_{b,a} = 0.02$, (●) $\sigma = \omega = 1$, (+) $\sigma = 0.54$, $\omega = 1$, (▼) $\sigma = 1$, $\omega = 0.54$, and (▲) $\sigma = \omega = 0.54$. The dashed line denotes the expectation if the branch points were randomly distributed. The curve with filled circles is from ref 9.

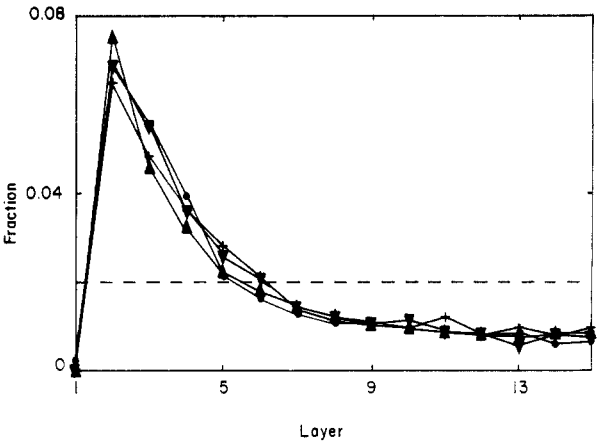

Figure 4. Fraction of lattice sites in each layer that are occupied by a branch end when $n_b = 2$, $f_{b,a} = 0.02$, (●) $\sigma = \omega = 1$, (+) $\sigma = 0.54$, $\omega = 1$, (▼) $\sigma = 1$, $\omega = 0.54$, and (▲) $\sigma = \omega = 0.54$. The dashed line denotes the expectation if the branch ends were randomly distributed. The curve with filled circles is from ref 9.

0.02 is the expectation in the event that the short branches are uniformly distributed throughout the lattice. When $\sigma = \omega = 1$, the actual result is close to the prediction for the horizontal dashed line for layer 5. There is an excess of short branches in layers 2–4 and a deficit in layers 6–15. The short branches with $n_b = 2$ tend to segregate in that portion of the amorphous region that is close to a crystalline interface.

The remaining curves in Figures 3 and 4 show equivalent results from simulations in which either σ or ω, or both, have values smaller than 1. These changes in the intramolecular short-range interactions have surprisingly little influence on the distribution of the short branches. In every case, there is an excess of short branches in layers 2–4, a value in layers 5 and 6 that is in reasonable agreement with the exception for a uniform distribution, and a deficit of short branches in layers 7–15. The differences that can be seen are in the details rather than in the overall picture. (For example, the distribution of short branches is most strongly peaked in layer 2 when σ and ω are both less than 1.) Since the overall trend for the distribution of the short branches is the same in all four simulations, it is clear that the drive for segregation of the short branches near the interface cannot be strongly dependent on the energetics of the short-range intramolecular interactions. Instead, the con-

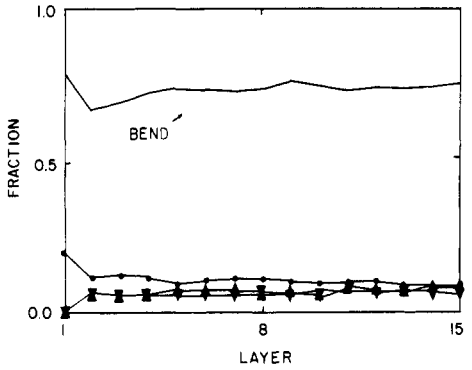

Figure 5. Fraction of bend bond pairs (top), parallel z bond pairs (middle), and parallel x and parallel y bond pairs (bottom) at beads in each layer when $n_b = 2$, $f_{b,a} = 0.02$, and $\sigma = \omega = 1$ (from ref 9).

stancy of the patterns in Figures 3 and 4 suggests that the segregation must be predominantly of entropic origin.

A similar pattern of segregation of the short branches is seen when $f_{b,a}$ is reduced from 0.02 to 0.01.

Simulations performed with markedly smaller values of ω than those used in Figures 3 and 4 are of little interest because the lattice becomes extensively ordered.

Growth of the Anisotropic Interfacial Region. On an isotropic cubic lattice, two bonds can meet at a given bead with bond angles of 90° or 180°. If the lattice is anisotropic because one direction is different from the other two, as is the case here, where the z direction is normal to the crystal interface and the x and y directions are parallel to the crystal interface, there may be different probabilities for consecutive collinear pairs of bonds oriented parallel to the z axis and those oriented perpendicular to the z axis. Figure 5 depicts the fraction of beads in each layer than have bond pairs that make a bend or bond pairs that make a bond angle of 180° and are parallel to the x, y, or z axis. The results are taken from Mathur et al.,[9] and they were obtained with $n_b = 2$, $f_{b,a} = 0.02$, and $\sigma = \omega = 1$. Bend bond pairs dominate over the others. Among the bond pairs with bond angles of 180°, there is a large excess of those parallel to the z axis in layer 1 and a smaller, but detectable, tendency for the result parallel to the z axis to exceed that parallel to the x or y axis at subsequent layers. Equivalent simulations without branches[9] (results not reproduced here) show a merger of the probabilities for bond pairs parallel to x, y, and z axes at layer 2. Therefore, the presence of the short branches produces an extension of the penetration into the lattice of the distinguishability of bond pairs parallel to the x, y, and z axes. From this result, we conclude that the segregation of the short branches is accompanied by an increase in the extent of the anisotropic interfacial region when $\sigma = \omega = 1$.

Figures 6 and 7 depict the occurrence of the different types of bond pairs when the simulation is repeated but with $\sigma = 0.54$. The values of $f_{b,a}$ are 0 and 0.02 in Figures 6 and 7, respectively. The change in the first-order intramolecular interaction energy has an influence on the occurrence of bond pairs with bond angles of 180° in both simulations, but the effect is much more dramatic in the presence of the short branches, Figure 7. They are now more prevalent than in the simulation with $\sigma = 1$, and, perhaps more importantly, there is a much greater distinction between those bond pairs oriented along the z axis and those oriented along either the x or y axis. Indeed, the influence of the crystalline interface extends throughout the entire lattice in Figure 7. A box with many more layers in the z direction than the 30 employed here would

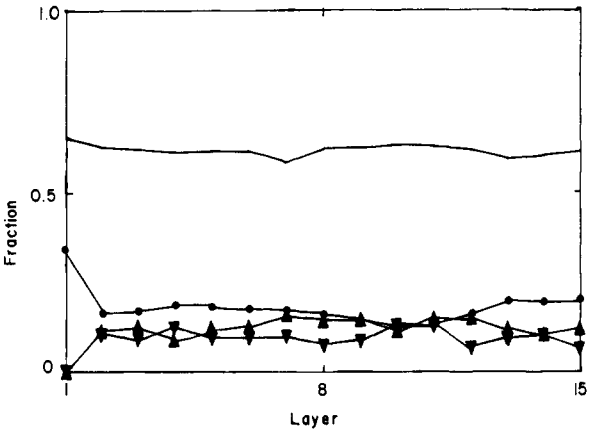

Figure 6. Fraction of bend bond pairs (top), parallel z bond pairs (middle), and parallel x and parallel y bond pairs (bottom) at beads in each layer when $f_{b,a} = 0$, $\sigma = 0.54$, and $\omega = 1$.

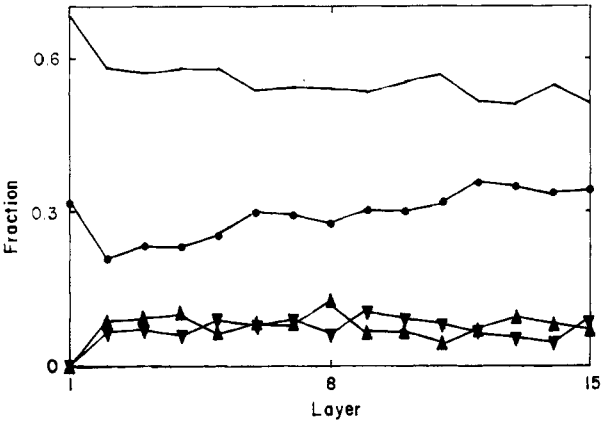

Figure 7. Fraction of bend bond pairs (top), parallel z bond pairs (middle), and parallel x and parallel y bond pairs (bottom) at beads in each layer when $n_b = 2$, $f_{b,a} = 0.02$, $\sigma = 0.54$, and $\omega = 1$.

be required in order to produce an isotropic region in the middle of the box. From this result, we can see that the anisotropic interfacial region will be much more extensive if there is a short-range preference for a locally extended conformation. This result is in marked contrast to the extent of segregation of the short branches, which is affected very little by the same change in the intramolecular short-range interactions, as shown in Figures 3 and 4.

A similar change in the energetics associated with a tight fold produces an effect that is qualitatively in the same direction, although much smaller in magnitude. This energetic term, which was denoted $E_\eta kT$ by Kumar and Yoon, has been shown by them to increase the extension of the anisotropic interfacial region in a lattice treatment of the system without branches.[16] Since the two effects are qualitatively in the same direction, in that they increase the distance into the lattice where the presence of the crystal causes the z direction to be distinguishable, they will act together if σ and ω are both less than 1.

Conclusion

The extension of the anisotropic interfacial region in lightly branched copolymers is sensitive to the nature of the intramolecular short-range interactions. The anisotropic interfacial region increases when these short-range interactions favor locally extended conformations. In contrast, the preference of short branches for that portion of the amorphous region near the crystal interface,

rather than the portion far removed from that interface, is much less sensitive to the intramolecular short-range interactions. Similar segregation of the short branches is seen in simulations with and without intramolecular energetic terms.

Acknowledgment. This research was supported by a grant from the donors of the Petroleum Research Fund, administered by the American Chemical Society, and by National Science Foundation Grant DMR 87-06166.

References and Notes

(1) Layman, P. L. *Chem. Eng. News* **1989**, March 6, 20.
(2) Flory, P. J. *Trans. Faraday Soc.* **1955**, *51*, 848.
(3) Richardson, M. J.; Flory, P. J.; Jackson, J. B. *Polymer* **1963**, *4*, 226.
(4) Baker, C. H.; Mandelkern, L. *Polymer* **1966**, *7*, 71.
(5) Alamo, R.; Domszy, R.; Mandelkern, L. *J. Phys. Chem.* **1984**, *88*, 6587.
(6) Voigt-Martin, I. G.; Alamo, R.; Mandelkern, L. *J. Polym. Sci., Polym. Phys. Ed.* **1986**, *24*, 1283.
(7) VanderHart, D. L.; Perez, E. *Macromolecules* **1986**, *19*, 1902.
(8) Mathur, S. C.; Mattice, W. L. *Macromolecules* **1988**, *21*, 1354.
(9) Mathur, S. C.; Rodrigues, K.; Mattice, W. L. *Macromolecules* **1989**, *22*, 2781.
(10) Guttman, C. M.; DiMarzio, E. A.; Hoffman, J. D. *Macromolecules* **1982**, *15*, 525.
(11) Abe, A.; Jernigan, R. L.; Flory, P. J. *J. Am. Chem. Soc.* **1966**, *88*, 631.
(12) Rodrigues, K.; Mathur, S. C.; Mattice, W. L. *Polym. Prepr. (Am. Chem. Soc., Div. Polym. Chem.)* **1989**, *30* (2), 275.
(13) Mansfield, M. L. *J. Chem. Phys.* **1982**, *77*, 1554.
(14) Mansfield, M. L. *Macromolecules* **1983**, *16*, 914.
(15) Metropolis, N.; Rosenbluth, A. W.; Rosenbluth, M. N.; Teller, A. H.; Teller, E. *J. Chem. Phys.* **1953**, *21*, 1087.
(16) Kumar, S. K.; Yoon, D. Y. *Macromolecules* **1989**, *22*, 3458.

Observation of a New High-Temperature Transition in Polytetrafluoroethylene

Yash P. Khanna,* Georgette Chomyn, Rakesh Kumar, N. Sanjeeva Murthy, Kennedy P. O'Brien, and Annemarie C. Reimschuessel

Research & Technology, Allied-Signal, Inc., Morristown, New Jersey 07962.
Received September 6, 1989; Revised Manuscript Received November 13, 1989

ABSTRACT: We wish to report that in sintered polytetrafluoroethylene (PTFE), there is an order → disorder transition at 370 ± 10 °C which otherwise has been known to show the highest temperature (melting) transition at 327 °C since its discovery over 50 years ago. The intensity of the 370 °C transition varies from sample to sample, and at present we are not fully aware of the factors responsible for its selective formation except that a high molecular weight and moderate shear stresses in the solid ↔ melt region are required. Limited experimental data available suggest that the loss of helical order occurs at ~327 °C and at ~370 °C the loss of equatorial order takes place; the latter existing in the presence of molecular constraint created from shear stresses on a high molecular weight resin. Differential scanning calorimetry, rheology, hot-stage optical microscopy, variable-temperature X-ray diffraction, and infrared data are presented to demonstrate these findings.

Introduction

The melting, crystallization, and morphology of PTFE and their relationship to molecular weight have been discussed in the papers of Suwa et al.[1,2] At a heating rate of 8 °C/min, their differential scanning calorimetry (DSC) results suggest a melting peak temperature (T_m) between 335 and 341 °C for the virgin PTFE. The sintered PTFE exhibits a T_m at 327 ± 1 °C. Wunderlich[3] claims an equilibrium melting temperature (T_m^0) of 327 °C for PTFE. Thus, although the T_m^0, i.e., melting of perfect crystals, is accepted to be 327 °C, depending upon the sample history and experimental conditions, one can come across a melting temperature as high as about 341 °C for PTFE as a result of superheating.[4] Recently we have commented upon the melting temperatures of PTFE, i.e., 327 vs 341 °C, and proposed a T_m^0 = 334 °C.[5] References 4 and 5 are recommended for a discussion of the superheating in PTFE.

On August 27, 1986, we became aware of an unusual high-temperature transition (melting) in PTFE at 370 °C (e.g. see Figure 1). As we are getting ready to send this paper, we have come across a reference by Grebowicz et al.[6] which mentions the 370 °C transition. The

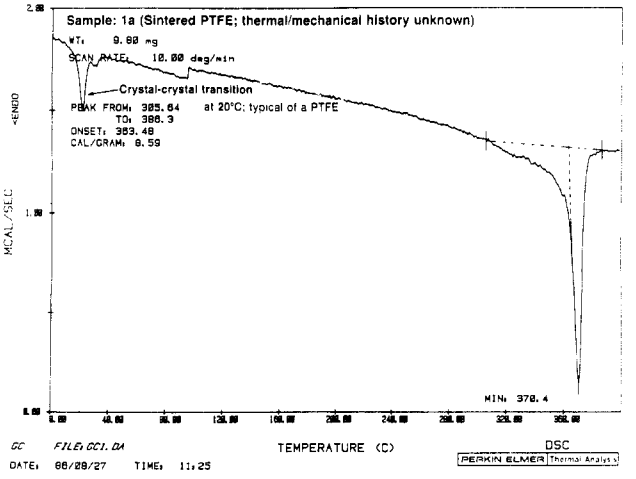

Figure 1. DSC thermogram (10 °C/min) showing the 370 °C transition in a sintered PTFE (sample 1a; thermal/mechanical history unknown).

major differences between Grebowicz et al.[6] and our studies are as follows: (1) they report only a trace peak at

0024-9297/90/2223-2488$02.50/0